

1 **TITLE**

2
3 Ferritin is required at multiple stages during the embryonic development of *Drosophila melanogaster*.
4

5 **AUTHORS**

6
7 Nicanor González-Morales^{1, 2}, Fanis Missirlis^{1, 3}, Miguel Ángel Mendoza-Ortíz¹, Liisa M. Blowes^{1, 4}
8 and Juan R. Riesgo-Escovar^{1*}
9

10 **AFFILIATIONS**

11
12 ¹ Departamento de Neurobiología del Desarrollo y Neurofisiología, Instituto de Neurobiología,
13 Universidad Nacional Autónoma de México, Campus UNAM Juriquilla, Querétaro, 76230, México.

14 ² CNRS, Institut de Biologie Valrose, iBV, UMR 7277, Nice, 06100, France.

15 ³ Departamento de Fisiología, Biofísica y Neurociencias, Centro de Investigación y de Estudios
16 Avanzados del Instituto Politécnico Nacional, Avenida IPN 2508, Zacatenco, México, Distrito Federal,
17 07360, México.

18 ⁴ School of Biological and Chemical Sciences, Queen Mary University of London, London, E1 4NS,
19 UK.
20

21 *corresponding author: riesgo@unam.mx
22

ABSTRACT

In *Drosophila*, iron is stored in the endomembrane system of cells inside a protein cavity formed by ferritin subunits of two types (Fer1HCH and Fer2LCH) in a 1:1 stoichiometry. Ferritin accumulates in the midgut, nervous system, hemolymph and nephrocytes of *Drosophila* larvae. Here, we show that mutation of either ferritin gene product or deletion of both genes resulted in a similar set of phenotypes of embryonic lethality, ranging from non-deposition of cuticle to developmental defects associated with germ band retraction, dorsal closure and head involution. Maternal contribution of ferritin, which varied reflecting the mother's iron stores, is used in early development, but zygotic ferritin mutants died with ectopic apoptotic events and disrupted intestinal morphology. The embryonic nervous system of ferritin mutants presented ventral nerve cord disruptions, misguided axonal projections and brain malformations. Finally, ferritin accumulation was also observed in embryonic hemocytes. One ferritin mutant showed no hemocyte ferritin accumulation and this expression was also lost by genetic inhibition of the secretory pathway. Our work suggests that insect ferritin functions in iron storage, intercellular iron transport and protection from oxidative stress at multiple times during the embryonic development of *Drosophila melanogaster*.

INTRODUCTION

Iron is the most abundant transition metal on earth, commonly found at the active sites of proteins in the form of heme or iron-sulfur clusters or as mono-nuclear and di-nuclear iron (Sheftel et al. 2012). Because of the high reactivity between iron and oxygen, iron has become a key player in aerobic metabolism but also catalyzes oxidative stress when present in excess. Therefore, iron concentration within subcellular compartments and in extracellular fluids is tightly regulated (Cabantchik 2014). The Divalent Metal Transporter 1 (DMT1) is responsible for cellular iron uptake (Gunshin et al. 1997). Ferritin participates in iron homeostasis as the main iron storage complex in both prokaryotes and eukaryotes (Harrison & Arosio 1996). The major form of ferritin in vertebrate animals is cytosolic and consists of 24 subunits of H and L protein chains that assemble into a cage-like structure that sequesters up to 4,500 atoms of iron in its interior core. The H chain contains a ferroxidase center necessary for iron internalization while the L chain contains acidic groups exposed in the interior surface of holoferritin facilitating iron mineralization (Santambrogio et al. 1993). Ferritin genes are regulated during translation by the binding of an iron regulatory protein (IRP) to an iron responsive element (IRE) located in the 5' untranslated region of the mRNA (Pantopoulos et al. 2012). The discovery in mice of ferritin receptors Scara5 (Li et al. 2009) and Tim2 (Todorich et al. 2008) has lead to the idea that ferritin might be involved in iron transport (Meyron-Holtz et al. 2011), however this idea remains controversial (Kell & Pretorius 2014).

In insects, ferritin shells have an H₁₂L₁₂ organization due to inter- and intra- subunit disulfide-bonds ensuring protein folding and assembly (Hamburger et al. 2005). Ferritin intracellular localization in most insects is directed to the endoplasmic reticulum and the Golgi (Missirlis et al. 2006; Missirlis et al. 2007). The *Drosophila melanogaster* genome encodes for three ferritin genes: *Ferritin 1 heavy chain homologue (Fer1HCH)* and *Ferritin 2 light chain homologue (Fer2LCH)* together produce the major ferritin complex (Georgieva et al. 2002; Georgieva et al. 1999; Mandilaras et al. 2013), whereas *Ferritin 3 heavy chain homologue (Fer3HCH)* encodes the mitochondrial ferritin, which is predominantly expressed in testis (Kumar et al. 2011; Missirlis et al. 2006). The *Drosophila* Iron Regulatory Protein-1A (IRP-1A), in its iron-sulfur cluster depleted modality, binds IREs thereby regulating the translation of a subset of *Fer1HCH* mRNA transcripts (Lind et al. 2006). The sole *Drosophila* DMT1 homolog (Folwell et al. 2006) was originally isolated as a gustatory mutant named

Malvolio (Mvl) (D'Souza et al. 1999). Previous work has shown that ferritin is required for embryonic and larval development (Missirlis et al. 2007; Tang & Zhou 2013) and that the ferroxidase center of the H chain is essential (Missirlis et al. 2007), but the specific phenotypes of the ferritin mutants have not been studied to date. *Drosophila* ferritin has been proposed to function as an external source of iron (Li 2010; Nichol et al. 2002; Tang & Zhou 2013; Zhou et al. 2007) but functional analysis in support of this proposition exists only for the secreted ferritin of ticks (Galay et al. 2013; Galay et al. 2014; Hajdusek et al. 2009).

Here, we analyze *Fer1HCH* and *Fer2LCH* mutant embryonic phenotypes. We propose that key functions of the ferritin subunits are likely mediated through the ferritin complex, as their respective mutant phenotypes are indistinguishable during embryogenesis. We show that ferritin mutant phenotypes can be enhanced when embryos are deprived of or have a reduced ferritin maternal contribution, by induction of germ line clones or by limiting iron uptake in parental diets, respectively. A severe central nervous system (CNS) defect, ectopic apoptosis and intestinal damage are seen in embryos dying at later stages of development. Blocking the intracellular secretory pathway during embryogenesis results in the mislocalisation of ferritin. We hypothesize that failure of ferritin transport in one of the mutants tested contributes to the resulting phenotype and lethality.

RESULTS AND DISCUSSION

Pleiotropic phenotypes of ferritin mutants revealed from embryonic cuticle preparations

To characterize the embryonic lethal phenotype of ferritin mutants we analyzed the cuticles of previously described transposon-induced loss-of-function alleles *Fer1HCH*⁴⁵¹ and *Fer2LCH*³⁵ (Missirlis et al. 2007; Tang & Zhou 2013), a null mutation for both ferritin genes *Df(3R)Fer* (Gutierrez et al. 2013), a GFP-trap line *Fer1HCH*^{G188} (Missirlis et al. 2007) and also a new allele described here for the first time *Fer2LCH*⁴¹⁷, which fails to complement *Fer1HCH*⁴⁵¹, *Fer1HCH*^{G188} and *Fer2LCH*³⁵ (see Materials and Methods). Cuticle preparations of ferritin mutants revealed examples of developmental arrest during the key embryonic processes of germ band extension and retraction, dorsal closure and head involution (Figure 1). Nevertheless, quantification of phenotypes suggests that most

mutant embryos presented either a normal cuticle (~75%) or no cuticle at all (~15%). These phenotypes suggested that ferritin is required multiple times during development, consistent with differential requirements for iron to support the metabolic shifts that occur during development (Tennessen et al. 2014). Notably, a number of iron sulfur cluster proteins are induced during the final stages of embryogenesis to support aerobic glycolysis.

A maternal contribution of ferritin is utilized during early embryonic development

Ferritin is maternally contributed (Missirlis et al. 2007). We therefore wondered if our analysis of zygotic mutants could miss early requirements for ferritin fulfilled by this maternal contribution. To analyze how maternal ferritin functioned during embryogenesis we followed two strategies: curtailing iron availability in mothers and generating female germ line clones without ferritin. One way of reducing ferritin expression in adults is to add an iron-specific chelator in their diet (Gutierrez et al. 2013; Missirlis et al. 2006). We hypothesized that reduced overall ferritin levels would result in decreased ferritin maternal contribution and a more severe embryonic phenotype. Homozygous mutant embryos derived from heterozygous adults grown with food containing 200μM Bathophenanthroline Sulfate (BPS) showed a doubling of incidence for the no cuticle phenotype (from ~15% to ~30%; Figure 1). Lack of cuticle deposition was likely due to early embryonic death before epidermal differentiation, although we have not excluded a particular requirement for iron in the differentiation of the epidermis, which could provide an alternative explanation for the same phenotypic outcome. Late embryonic phenotypes also became more frequent: U-shaped embryos, indicative of a failure to retract the germ band, augmented from ~2% to ~4%, and embryos failing to complete dorsal closure increased from ~1% to ~4% (Figure 1F; BPS columns). At the same time, the percentage of “wild type” cuticles decreased. This evidence shows that the extent of ferritin maternal contribution is at least partially regulated in flies *via* limited iron availability. We note that the changes in phenotypic classes abundances were consistently similar in *Fer1HCH*⁴⁵¹, *Fer2LCH*³⁵, and *Df(3R)Fer*. Feeding extra iron to adults did not result in a rescue of the embryonic phenotype of the mutant offspring (Figure 1F, FAC), even though total levels of ferritin in mothers were increased, showing that maternal ferritin contribution was not sufficient to fully rescue embryogenesis.

To further explore whether maternal ferritin was partially rescuing zygotic ferritin mutants, especially

during early development, we generated homozygous mutant germ line clones for the ferritin genes. Most germ line clones had no cuticle or bore cuticles with defects. The 'no cuticle' phenotype percentage changed spectacularly from ~15% to ~80% (Figure 1F). Heterozygous embryos without maternal contribution developed normally into adults (data not shown). We hypothesize that this rescue was due to zygotic ferritin genes being overexpressed as a response to lack of maternal ferritin and that iron in these embryos was delivered to the developing oocyte by other means.

Central Nervous System (CNS) phenotypes of ferritin mutants

The majority of zygotic ferritin mutant embryos derived from heterozygous mothers died at the final stages of embryogenesis with an apparently normal cuticle. Therefore, we sought to study internal tissues that might be affected by lack of ferritin. Since ferritin protein in first instar larvae is concentrated in the intestine and the CNS (Mehta et al. 2009), we asked whether the CNS developed normally in ferritin mutants. We performed immunofluorescence with antibodies against neuronal markers. The application of an antibody against Elav, which marks all neuronal nuclei, revealed that ferritin mutants harbor holes in the abdominal segments of the CNS (Figure 2). More severe phenotypes were also present, albeit in fewer embryos, including aberrant condensation of the CNS, twisted CNS, and complete lack of parts of the brain and peripheral nervous system (PNS). Importantly, and consistent with our analysis of the cuticle phenotypes discussed above, these phenotypes were observed with both ferritin alleles and with the 2.2 kb genomic deletion that specifically deletes both *Fer1HCH* and *Fer2LCH* (Figure 2). We interpret this to mean that, in wild type embryos individual ferritin subunits function in concert to assemble the ferritin complex and do not carry out subunit-specific functions.

It was previously reported that in adult flies, RNA interference in subsets of neurons against *Fer2LCH* but not against *Fer1HCH* disrupted circadian rhythms (Mandilaras & Missirlis 2012). Furthermore, some cell types, including commonly used cell culture lines (Metzendorf et al. 2009; Missirlis et al. 2003a), only express *Fer1HCH* and not *Fer2LCH*. Finally, overexpression of either *Fer1HCH* or *Fer2LCH* or both subunits simultaneously in *Drosophila* glia (Kosmidis et al. 2011) or neurons (Wu et al. 2012b) resulted in qualitatively different responses. Thus, the question of how each cell type regulates the two ferritin genes and subunits and whether they always act in concert, as the analysis of

mutant embryonic phenotypes suggests, requires further investigation.

Further markers were used in embryos homozygous for *Df(3R)Fer*. We tested whether neuronal axons were projecting normally using α -BP102, which stains axons. BP102-dependent fluorescence revealed that CNS axons are frequently misguided (Figure 3A, D). The developing CNS consists of at least four types of cells: neuroblasts, ganglion mother cells, neurons and glia. Neuroblasts give rise to ganglion mother cells, and these, in turn, give rise to neurons and glia (Biffar & Stollewerk 2014). In order to test whether neuroblasts were affected in ferritin mutant embryos, we performed antibody staining with Deadpan and Evenskipped (Eve) antibodies (Boone & Doe 2008; Kohwi et al. 2013). Our preparations with antibodies against Deadpan, which marks all neuroblasts, indicate that CNS defects are already present within neuroblast cell lineages, including misplaced neuroblasts (Figure 3B, E). As expected for early CNS defects, Eve positive neuroblasts were also heavily misplaced (Figure 3C, F). In conclusion, the developing CNS of embryos lacking the ferritin genes is affected from the time neuroblast cell lineages are specified giving rise to contorted and aberrant CNS in late embryos.

A ferritin enhancer trap shows expression in the CNS

*Fer1HCH*⁴⁵¹ carries a *LacZ* element that serves as reporter of *Fer1HCH* expression. To test whether this reporter recapitulates known changes in *Fer1HCH* expression, we monitored *LacZ* activity in the anterior midgut upon iron feeding of larvae, as occurs for endogenous *Fer1HCH* (Figure S1). Iron-dependent induction of expression was confirmed with this reporter and we therefore used *LacZ* detection to monitor *Fer1HCH* expression in the embryo. *LacZ* driven from *Fer1HCH*⁴⁵¹ is strongly expressed in the neuroectoderm (Figure 4A). The co-localization between the neuronal marker *Elav* and the β -galactosidase reporter was also observed in homozygous mutant embryos with a disrupted CNS (Figure 4B). We note that the use of the *Elav-Gal4* driver to silence either *Fer1HCH* or *Fer2LCH* resulted in viable adults with disturbed circadian behavior (Mandilaras & Missirlis 2012) and apparent neurodegeneration (Tang & Zhou 2013). RNA interference is known to cause reduced expression but not complete silencing of its targets, which may explain why the RNAi flies survived to adulthood. In addition, overexpression of ferritin subunits with *Elav-Gal4* failed to rescue their respective mutants (Tang & Zhou 2013). Nevertheless, our findings suggest that ferritin is expressed in the embryonic CNS and is required for its development.

Ectopic apoptotic activation in ferritin mutants

Several links have been drawn in the last decade between iron metabolism and apoptosis (Gambis et al. 2011; Kosmidis et al. 2011; Pham et al. 2004). We hypothesized that the disrupted CNS would result following cell death by an apoptotic mechanism. To test the hypothesis we used an antibody that recognizes solely the cleaved, activated caspases, and has been used in flies to mark apoptotic cells (Denton et al. 2008). In contrast to control embryos at stage 12 where there was no apoptotic signal detected (Figure 5A), ectopic apoptotic activation appeared in the neuroectoderm region in mutant embryos (Figure 5B). By stage 15 of embryogenesis control embryos have a weak and restricted apoptotic signal (Figure 5C) whereas in the mutant embryos this signal was massive and covered most of the embryo (Figure 5D). Similar widespread immunoreactivity against activated caspase was also observed with *Fer1HCH*⁴⁵¹ and *Fer2LCH*³⁵ homozygous mutant embryos (data not shown). Thus, the early apoptotic activation seen in ferritin mutants, mainly restricted to the neuroectoderm region, suggests that the CNS may be more susceptible to the lack of the ferritin complex, although, ultimately, many other tissues become affected.

The *Drosophila* DMT1 homolog, *Malvolio*, is upregulated in ferritin mutants

Mutations in *Mvl* result in reduced iron within intestinal iron storage cells and in the whole body (Bettendi et al. 2011). *Mvl* mutants can suppress both intestinal iron accumulation resulting from ferritin (*Tang & Zhou 2013*) and Multicopper Oxidase-1 (MCO1) (Lang et al. 2012) misregulation. MCO1 catalyzes the oxidation of ferrous iron (Fe²⁺) to ferric iron (Fe³⁺) and is thought to participate in cellular iron export in insects (Lang et al. 2012). In view of the above findings, we used *Mvl*^{97f}, a P-element insertion mutant carrying *LacZ* reporter gene activity (Rodrigues et al. 1995) to assess β -Galactosidase activity staining. In control embryos, *LacZ* showed a very restricted pattern of *Mvl* expression consistent with previous studies (Kumar et al. 2011; Rodrigues et al. 1995), however in the absence of ferritin, *Mvl*-driven *LacZ* is upregulated (Figure 6A). We hypothesize that in the absence of functional ferritin, iron depleted cells upregulate *Mvl*. Strikingly, the addition of one copy of *Mvl*^{97f} hypomorphic allele into a ferritin-depleted embryo resulted in the appearance of melanotic spots, which were never observed in *Mvl*^{97f} or in ferritin homozygous mutants alone (Figure 6B, C). The interaction between

DMT1 and ferritin is reminiscent of the recent finding that the mammalian ferritin receptor SCARA5 is likewise up regulated in the absence of transferrin receptor (Li et al. 2009).

Ferritin expression, localization and trafficking during development

Fer1HCH^{G188} is a mutant *Fer1HCH* allele, shown to generate a chimeric GFP-Fer1HCH that faithfully mimics endogenous Fer1HCH pattern in heterozygous condition (Gutierrez et al. 2010; Mehta et al. 2009; Missirlis et al. 2007; Uhrigshardt et al. 2013). During stages 16-17 of embryonic development GFP tagged Fer1HCH is present in hemocytes (Figure 7A). Hemocytes are large cells that are loosely associated with peripheral tissues and can circulate in the hemolymph, where they function as both phagocytic and immune cells (Evans & Wood 2011). In order to confirm that the large, ferritin-accumulating cells were actually hemocytes we used Cg-Gal4 line to drive expression, exclusively in hemocytes, of a nuclearRFP in *Fer1HCH^{G188/+}* embryos (Figure 7A). GFP-Fer1HCH is present in the same cells as Cg-nRFP, but not in FB-nRFP (Figure 7B), where mRNA expression is seen (Missirlis et al. 2007). The GFP tag is thought to block the correct function of ferritin in homozygous *Fer1HCH^{G188}* embryos, because if all the H-subunits carry a GFP tag, embryonic development fails (Missirlis et al. 2007) and even *Fer1HCH^{G188/+}* flies show a mild reduction in iron accumulation within ferritin (Gutierrez et al. 2013). We noticed that homozygous mutant *Fer1HCH^{G188}* embryos showed a dramatically reduced expression of GFP-Fer1HCH than similarly staged heterozygous *Fer1HCH^{G188}* embryos (Figure 7E, F). Lower and restricted GFP-Fer1HCH expression in homozygous *Fer1HCH^{G188}* embryos, mainly seen in the intestinal region (Figure 7F), suggested either degradation of the mutant protein or that mutant, non-functional heteropolymers (composed exclusively of GFP-Fer1HCH and Fer2LCH subunits) would not be trafficked. Furthermore, we noted that the intestinal morphology of homozygous *Fer1HCH^{G188}* was affected (Figure 7F). To test further whether ferritin is delivered to hemocytes from other embryonic tissues and whether ferritin trafficking can be observed, we blocked the intracellular secretory pathway by means of a lethal mutation in *Sec23*, *sec23^{j13C8}*, a P-element insertion in the 5' UTR of *sec23*, expected to eliminate or severely attenuate gene function (Abrams & Andrew 2005). If ferritin is indeed transported during embryogenesis, blocking the secretory pathway will impede its exit from the cell where it was originally transcribed. Ferritin was not detected in hemocytes of *sec23^{j13C8/j13C8}* mutants; rather, GFP-Fer1HCH aggregates were detected mainly around the midgut (Figure 7D) in a similar expression pattern as observed in homozygous *Fer1HCH^{G188}*

mutants. Thus, in embryos impaired in the secretory pathway hemocytes fail to accumulate ferritin, suggesting that its source in wild type embryos may come from hemolymph ferritin. Taken together, our observations suggest that ferritin traffics between tissues during embryonic development and that the hemocytes could play a key role during this trafficking process, by importing ferritin from one tissue and delivering it to another. Such a communicating role for hemocytes has been previously suggested in the context of tissue communication in the innate immune response (Wu et al. 2012a).

Conclusions

Insect embryos must course through development with limited amounts of iron, provided during oogenesis by the mother in part via ferritin. It seems reasonable to assume that tissues developing at different rates and with different metabolic states present different iron requirements. Therefore, iron storage and transport are of vital importance for normal development. Ferritin appears to be serving both functions in *Drosophila*.

EXPERIMENTAL PROCEDURES

Fly stocks

As a control strain *y,w* flies were used. *Fer1HCH*⁴⁵¹ and *Fer2LCH*³⁵ are P(ry[+t7.2]=PZ) insertion alleles generated during a large-scale mutagenesis screen (Spradling et al. 1999), they have been partially characterized elsewhere (Missirlis et al. 2007) and they were obtained from the Bloomington Drosophila Stock Center (BDSC) stock numbers #11497 and #11483, respectively. *Fer2LCH*^{A17} was generated from an imprecise excision of *Fer2LCH*^{EP1059} (described in Flybase) and interferes with expression of both genes, as confirmed by complementation crosses. *Df(3R)Fer* was a gift from Alexis Gambis, Bertrand Mollereau and Hermann Steller and is a 2,2 kb deletion disrupting specifically *Fer1HCH* and *Fer2LCH* (Gutierrez et al. 2013). To generate germline clones, *Fer1HCH*⁴⁵¹ and *Fer2LCH*³⁵ were recombined unto FRT82 containing chromosomes (Xu & Rubin 1993). *Fer1HCH*^{G188} is a protein trap line and has been extensively described elsewhere (Missirlis et al. 2007). *Mvl*^{97f} is an homozygous viable a *P(lacW)* insertion was obtained from BDSC #5151 (Rodrigues et al. 1995).

287 *Sec23*^{j13c8} mutant is a *P(lacW)* insertion within the 5'UTR of *Sec23* (Abrams & Andrew 2005), BDSC
288 stock #10218. *Cg-Gal4* (BDSC stock #7011) was used to drive expression in the hemocytes, *drm-Gal4*
289 (BDSC stock #7098) in embryonic gut and scattered cells around the epidermis, *FB-Gal4* in the fat
290 bodies (Missirlis et al. 2006; Missirlis et al. 2003b). In cases where recombinant or double balanced
291 stocks were needed they were generated following conventional crossing schemes.

292

293 **Iron diets**

294

295 Flies were raised for 3 successive generations on standard medium supplemented with 200 μ M
296 Bathophenanthrolinedisulfonic acid disodium salt (SIGMA #B1375) referred to as BPS in the text or
297 with 1 mM ammonium iron (III) citrate (SIGMA #F5859) referred to as FAC. Adults were used for
298 embryo collections. Protein extracts from female adults were also analyzed by non-reducing SDS-
299 PAGE, confirming the differential accumulation of ferritin in flies raised on the respective diets (data
300 not shown).

301

302 **Immunohistochemistry and confocal imaging**

303

304 Following dechoriation with a commercial bleach solution, embryos from overnight collections were
305 devitellinized and fixed in a 1:1 mixture of heptane and 36% formaldehyde for 5 minutes and then
306 washed in methanol. Embryos were then stored at -20 C or rehydrated, and used for staining. Primary
307 antibodies used were: rat α -Elav 1:100, mouse α -BP102 1:100, mouse α -Eve 1:100 (Developmental
308 Studies Hybridoma Bank); α -activated Caspase 3 1:100 (Cell Signaling); and rat α -Deadpan 1:2, a gift
309 from Cheng-Yu Lee. Secondary antibodies used were: Alexa flour 546 α -rat 1:100 (Santa Cruz
310 Biotechnology), Cy5 α -mouse 1:1000, Cy3 α -mouse 1:1000, FITC α -rabbit 1:1000 (Zymax). Signal
311 from α -deadpan staining was increased with the ABC kit from Vectastain. A 510 Meta confocal
312 microscope (Zeiss) was used for fluorescent imaging, and images were processed with Zeiss software
313 and ImageJ.

314

315 **Cuticle preparations and X-Gal staining**

316

317 Embryos were collected in agar containing plates for 12 hours and incubated for another 36 hours at

25°C. Viable first instar larvae were removed from cultures. The cuticles of unhatched (dead) embryos were dechorionated and mounted in Hoyer's medium and incubated for 24 hours at 50°C to digest soft tissues. Resulting cuticles were then viewed and photographed with dark field optics in a compound microscope (Nikon). For X-Gal staining embryos were fixed and stained with X-Gal using standard procedures. Both controls and experimental embryos were incubated in parallel for the same amount of time to allow for direct comparisons.

ACKNOWLEDGEMENTS

We thank María Teresa Peña-Rangel for expert technical assistance in the course of this project, Nydia Hernández-Rios for assistance with the use of the confocal microscope. We also acknowledge Cheng-Yu Lee for sending the α -deadpan antibody and Alexis Gambis, Bertrand Mollereau, Hermann Steller for sharing the *Df(3R)Fer* fly stock prior to publication.

FIGURE LEGENDS

Figure 1. Ferritin mutants result in a variety of cuticle phenotypes quantified by different colors. Examples are shown of (A) wild type cuticle (green), (B) head involution defects (red), (C) dorsal closure defects (yellow), (D) germ band retraction defects (orange), (E) no cuticle deposition (blue). (F) Percentages of cuticular phenotypes of ferritin mutants. An enhancement of the earlier phenotypes was seen in mutant embryos whose mothers were fed BPS. 80% of embryos derived from ferritin mutant germline clones failed to develop cuticle. C: normal diet, FAC: high iron diet, BPS: low iron diet, GL: germline clones, n: number of cuticles examined.

Figure 2. Ferritin mutants result in CNS phenotypes revealed by α -Elav immunofluorescence. All embryos were oriented with anterior to the left and were visualized from a ventrolateral view. (A) control *y, w* embryo, (B-D) three examples of *Fer1HCH⁴⁵¹*, (E, F) *Fer1HCH³⁵* and (G,H) *Df(3R)Fer* homozygous mutant embryos. The CNS appears twisted (C, E, H) and holes are seen within the ventral nerve cord (white arrows, B, D, F, H) in mutant embryos from all three genotypes.

Figure 3. In *Df(3R)Fer* homozygous mutant embryos the CNS appears contorted and with gaps in its organization. (A) Axons of the brain and ventral nerve cord have a stereotyped pattern in normal development. (B, C) Two different neuroblast populations, marked by Dpn and Eve, respectively, show a characteristic spatial organization in control *y, w* embryos. In homozygous *Df(3R)Fer* mutants, (D) the axons form but are disorganized and (E, F) the neuroblast populations are misplaced.

Figure 4. *Fer1HCH⁴⁵¹ lacZ* enhancer trap is expressed in the embryonic CNS. Using an antibody against β -Galactosidase (green) and an antibody against the neuronal marker Elav (red), colocalization is observed in (A) heterozygous *Fer1HCH^{451/+}* and (B) homozygous *Fer1HCH⁴⁵¹* embryos.

Figure 5. Ferritin mutants cause apoptosis in the CNS and other tissues. Whole embryos were treated with an α -CSP3act marking apoptotic cells (green), and an α -Elav marking neurons (red). (A) Absence of staining for CSP3act in stage 12 *y, w* embryos, whereas (B) apoptotic markers appear in homozygous *Df(3R)Fer* embryos from stage 12 onwards mostly restricted to the neurogenic region. C) At stage 15 limited apoptotic events are seen in *y, w* embryos. D) At stage 15 homozygous *Df(3R)Fer*

embryos apoptosis can be observed in all embryonic tissues. (E) Higher magnification of a control ventral nerve cord and (F) a hole in the ventral nerve cord. DAPI was used to mark nuclei (blue), α -Elav for neurons (red) and α -CSP3act (green) for apoptosis.

Figure 6. Genetic interaction between ferritin and the DMT1 homolog *Mvl*. (A) The *Mvl*^{97f}-*LacZ* line shows a spatially restricted expression pattern for *Mvl*, mainly in head region, the brain, and a segmental repeated pattern. (B) In a *Fer2LCH*^{Δ17} mutant background, *Mvl*^{97f}-*LacZ* expression is induced. Black arrows denote the head region, white asterisk the embryonic brain, red asterisk the ventral nerve cord, and red arrows mark the segmented expression pattern. Cuticle preparations of (C) a homozygous *Fer2LCH*^{Δ17} embryo and (D) a double mutant *Mvl*^{97f}, *Fer2LCH*^{Δ17}. (E) Quantification of the appearance of melanotic spots in the cuticle following the introduction of one or two *Mvl*^{97f} alleles into a ferritin mutant background.

Figure 7. Ferritin accumulation in embryos with different genetic backgrounds. Ferritin protein was visualized in all embryos from the *Fer1HCH*^{G188} GFP trap line. In stage 17 heterozygous *Fer1HCH*^{G188/+} embryos that successfully complete development, ferritin mainly accumulates in the midgut and in hemocytes. (A) The GFP-Fer1HCH signal is found in hemocytes marked by *cg>nRFP*, but not (B) in the fat bodies marked by *FB>nRFP*. (C, D) Blocking the secretory pathway using a homozygous mutant *Sec23*^{j13C8} background reveals that ferritin is absent from the hemocytes, where it normally resides, but accumulates in intestine. (E, F) *Fer1HCH*^{G188} homozygous embryos, which die like other ferritin mutants, also show ferritin accumulation in the intestine. These embryos also lose *drm>nRFP* staining suggesting intestinal disruption and lack ferritin accumulation in hemocytes suggesting ferritin trafficking defects.

Figure S1. *Fer1HCH*^{Δ51} is a functional ferritin enhancer trap line. β -Galactosidase expression is normally restricted to the iron region in the larval midgut but if the expression is enhanced in the anterior midgut (AMG) when iron fed, as occurs in wild type larve (Mehta et al. 2009).

394 REFERENCES

- 395
- 396 Abrams EW, and Andrew DJ. 2005. CrebA regulates secretory activity in the *Drosophila* salivary
- 397 gland and epidermis. *Development* 132:2743-2758.
- 398 Bettedi L, Aslam MF, Szular J, Mandilaras K, and Missirlis F. 2011. Iron depletion in the intestines of
- 399 Malvolio mutant flies does not occur in the absence of a multicopper oxidase. *J Exp Biol*
- 400 214:971-978.
- 401 Biffar L, and Stollewerk A. 2014. Conservation and evolutionary modifications of neuroblast
- 402 expression patterns in insects. *Dev Biol* 388:103-116.
- 403 Boone JQ, and Doe CQ. 2008. Identification of *Drosophila* type II neuroblast lineages containing
- 404 transit amplifying ganglion mother cells. *Dev Neurobiol* 68:1185-1195.
- 405 Cabantchik ZI. 2014. LABILE IRON IN CELLS AND BODY FLUIDS . Physiology, Pathology and
- 406 Pharmacology. *Frontiers in Pharmacology* 5.
- 407 D'Souza J, Cheah PY, Gros P, Chia W, and Rodrigues V. 1999. Functional complementation of the
- 408 malvolio mutation in the taste pathway of *Drosophila melanogaster* by the human natural
- 409 resistance-associated macrophage protein 1 (Nramp-1). *J Exp Biol* 202:1909-1915.
- 410 Denton D, Mills K, and Kumar S. 2008. Methods and protocols for studying cell death in *Drosophila*.
- 411 *Methods Enzymol* 446:17-37.
- 412 Evans IR, and Wood W. 2011. *Drosophila* embryonic hemocytes. *Curr Biol* 21:R173-174.
- 413 Folwell JL, Barton CH, and Shepherd D. 2006. Immunolocalisation of the *D. melanogaster* Nramp
- 414 homologue Malvolio to gut and Malpighian tubules provides evidence that Malvolio and
- 415 Nramp2 are orthologous. *J Exp Biol* 209:1988-1995.
- 416 Galay RL, Aung KM, Umemiya-Shirafuji R, Maeda H, Matsuo T, Kawaguchi H, Miyoshi N, Suzuki H,
- 417 Xuan X, Mochizuki M, Fujisaki K, and Tanaka T. 2013. Multiple ferritins are vital to
- 418 successful blood feeding and reproduction of the hard tick *Haemaphysalis longicornis*. *J Exp*
- 419 *Biol* 216:1905-1915.
- 420 Galay RL, Umemiya-Shirafuji R, Bacolod ET, Maeda H, Kusakisako K, Koyama J, Tsuji N, Mochizuki
- 421 M, Fujisaki K, and Tanaka T. 2014. Two kinds of ferritin protect ixodid ticks from iron
- 422 overload and consequent oxidative stress. *PLoS One* 9:e90661.
- 423 Gambis A, Dourlen P, Steller H, and Mollereau B. 2011. Two-color in vivo imaging of photoreceptor
- 424 apoptosis and development in *Drosophila*. *Dev Biol* 351:128-134.
- 425 Georgieva T, Dunkov BC, Dimov S, Rakhev K, and Law JH. 2002. *Drosophila melanogaster* ferritin:
- 426 cDNA encoding a light chain homologue, temporal and tissue specific expression of both
- 427 subunit types. *Insect Biochem Mol Biol* 32:295-302.
- 428 Georgieva T, Dunkov BC, Harizanova N, Rakhev K, and Law JH. 1999. Iron availability dramatically
- 429 alters the distribution of ferritin subunit messages in *Drosophila melanogaster*. *Proc Natl*
- 430 *Acad Sci U S A* 96:2716-2721.
- 431 Gunshin H, Mackenzie B, Berger UV, Gunshin Y, Romero MF, Boron WF, Nussberger S, Gollan JL,
- 432 and Hediger MA. 1997. Cloning and characterization of a mammalian proton-coupled
- 433 metal-ion transporter. *Nature* 388:482-488.
- 434 Gutierrez L, Sabaratnam N, Aktar R, Bettedi L, Mandilaras K, and Missirlis F. 2010. Zinc
- 435 accumulation in heterozygous mutants of fumble, the pantothenate kinase homologue of
- 436 *Drosophila*. *FEBS Lett* 584:2942-2946.
- 437 Gutierrez L, Zubow K, Nield J, Gambis A, Mollereau B, Lazaro FJ, and Missirlis F. 2013. Biophysical
- 438 and genetic analysis of iron partitioning and ferritin function in *Drosophila melanogaster*.

439 *Metallomics* 5:997-1005.

440 Hajdusek O, Sojka D, Kopacek P, Buresova V, Franta Z, Sauman I, Winzerling J, and Grubhoffer L.

441 2009. Knockdown of proteins involved in iron metabolism limits tick reproduction and

442 development. *Proc Natl Acad Sci U S A* 106:1033-1038.

443 Hamburger AE, West AP, Jr., Hamburger ZA, Hamburger P, and Bjorkman PJ. 2005. Crystal

444 structure of a secreted insect ferritin reveals a symmetrical arrangement of heavy and light

445 chains. *J Mol Biol* 349:558-569.

446 Harrison PM, and Arosio P. 1996. The ferritins: molecular properties, iron storage function and

447 cellular regulation. *Biochim Biophys Acta* 1275:161-203.

448 Kell DB, and Pretorius E. 2014. Serum ferritin is an important inflammatory disease marker, as it

449 is mainly a leakage product from damaged cells. *Metallomics*.

450 Kohwi M, Lupton JR, Lai SL, Miller MR, and Doe CQ. 2013. Developmentally regulated subnuclear

451 genome reorganization restricts neural progenitor competence in *Drosophila*. *Cell* 152:97-

452 108.

453 Kosmidis S, Botella JA, Mandilaras K, Schneuwly S, Skoulakis EM, Rouault TA, and Missirlis F. 2011.

454 Ferritin overexpression in *Drosophila* glia leads to iron deposition in the optic lobes and

455 late-onset behavioral defects. *Neurobiol Dis* 43:213-219.

456 Kumar S, Konikoff C, Van Emden B, Busick C, Davis KT, Ji S, Wu LW, Ramos H, Brody T,

457 Panchanathan S, Ye J, Karr TL, Gerold K, McCutchan M, and Newfeld SJ. 2011. FlyExpress:

458 visual mining of spatiotemporal patterns for genes and publications in *Drosophila*

459 embryogenesis. *Bioinformatics* 27:3319-3320.

460 Lang M, Braun CL, Kanost MR, and Gorman MJ. 2012. Multicopper oxidase-1 is a ferroxidase

461 essential for iron homeostasis in *Drosophila melanogaster*. *Proc Natl Acad Sci U S A*

462 109:13337-13342.

463 Li JY, Paragas N, Ned RM, Qiu A, Viltard M, Leete T, Drexler IR, Chen X, Sanna-Cherchi S,

464 Mohammed F, Williams D, Lin CS, Schmidt-Ott KM, Andrews NC, and Barasch J. 2009.

465 Scara5 is a ferritin receptor mediating non-transferrin iron delivery. *Dev Cell* 16:35-46.

466 Li S. 2010. Identification of iron-loaded ferritin as an essential mitogen for cell proliferation and

467 postembryonic development in *Drosophila*. *Cell Res* 20:1148-1157.

468 Lind MI, Missirlis F, Melefors O, Uhrigshardt H, Kirby K, Phillips JP, Soderhall K, and Rouault TA.

469 2006. Of two cytosolic aconitases expressed in *Drosophila*, only one functions as an iron-

470 regulatory protein. *J Biol Chem* 281:18707-18714.

471 Mandilaras K, and Missirlis F. 2012. Genes for iron metabolism influence circadian rhythms in

472 *Drosophila melanogaster*. *Metallomics* 4:928-936.

473 Mandilaras K, Pathmanathan T, and Missirlis F. 2013. Iron absorption in *Drosophila melanogaster*.

474 *Nutrients* 5:1622-1647.

475 Mehta A, Deshpande A, Bettedi L, and Missirlis F. 2009. Ferritin accumulation under iron scarcity in

476 *Drosophila* iron cells. *Biochimie* 91:1331-1334.

477 Metzendorf C, Wu W, and Lind MI. 2009. Overexpression of *Drosophila* mitoferrin in l(2)mbn cells

478 results in dysregulation of Fer1HCH expression. *Biochem J* 421:463-471.

479 Meyron-Holtz EG, Moshe-Belizowski S, and Cohen LA. 2011. A possible role for secreted ferritin in

480 tissue iron distribution. *J Neural Transm* 118:337-347.

481 Missirlis F, Holmberg S, Georgieva T, Dunkov BC, Rouault TA, and Law JH. 2006. Characterization of

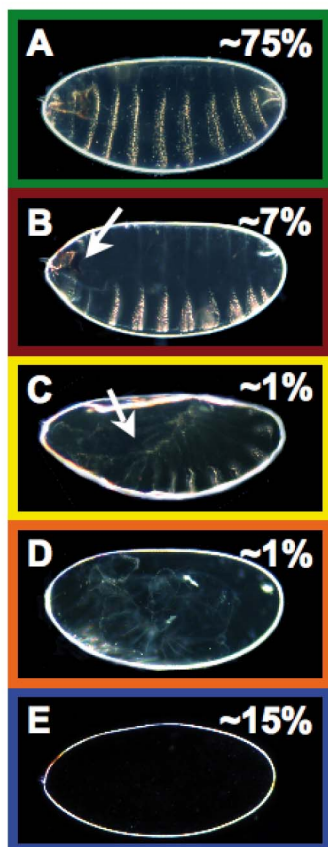
482 mitochondrial ferritin in *Drosophila*. *Proc Natl Acad Sci U S A* 103:5893-5898.

483 Missirlis F, Hu J, Kirby K, Hilliker AJ, Rouault TA, and Phillips JP. 2003a. Compartment-specific

484 protection of iron-sulfur proteins by superoxide dismutase. *J Biol Chem* 278:47365-47369.

- 485 Missirlis F, Kosmidis S, Brody T, Mavrakakis M, Holmberg S, Odenwald WF, Skoulakis EM, and Rouault
486 TA. 2007. Homeostatic mechanisms for iron storage revealed by genetic manipulations and
487 live imaging of *Drosophila* ferritin. *Genetics* 177:89-100.
- 488 Missirlis F, Rahlfs S, Dimopoulos N, Bauer H, Becker K, Hilliker A, Phillips JP, and Jackle H. 2003b. A
489 putative glutathione peroxidase of *Drosophila* encodes a thioredoxin peroxidase that
490 provides resistance against oxidative stress but fails to complement a lack of catalase activity.
491 *Biol Chem* 384:463-472.
- 492 Nichol H, Law JH, and Winzerling JJ. 2002. Iron metabolism in insects. *Annu Rev Entomol* 47:535-
493 559.
- 494 Pantopoulos K, Porwal SK, Tartakoff A, and Devireddy L. 2012. Mechanisms of mammalian iron
495 homeostasis. *Biochemistry* 51:5705-5724.
- 496 Pham CG, Bubici C, Zazzeroni F, Papa S, Jones J, Alvarez K, Jayawardena S, De Smaele E, Cong R,
497 Beaumont C, Torti FM, Torti SV, and Franzoso G. 2004. Ferritin heavy chain upregulation by
498 NF-kappaB inhibits TNFalpha-induced apoptosis by suppressing reactive oxygen species.
499 *Cell* 119:529-542.
- 500 Rodrigues V, Cheah PY, Ray K, and Chia W. 1995. malvolio, the *Drosophila* homologue of mouse
501 NRAMP-1 (Bcg), is expressed in macrophages and in the nervous system and is required
502 for normal taste behaviour. *EMBO J* 14:3007-3020.
- 503 Santambrogio P, Levi S, Cozzi A, Rovida E, Albertini A, and Arosio P. 1993. Production and
504 characterization of recombinant heteropolymers of human ferritin H and L chains. *J Biol*
505 *Chem* 268:12744-12748.
- 506 Sheftel AD, Mason AB, and Ponka P. 2012. The long history of iron in the Universe and in health
507 and disease. *Biochim Biophys Acta* 1820:161-187.
- 508 Spradling AC, Stern D, Beaton A, Rhem EJ, Lavery T, Mozden N, Misra S, and Rubin GM. 1999. The
509 Berkeley *Drosophila* Genome Project gene disruption project: Single P-element insertions
510 mutating 25% of vital *Drosophila* genes. *Genetics* 153:135-177.
- 511 Tang X, and Zhou B. 2013. Ferritin is the key to dietary iron absorption and tissue iron
512 detoxification in *Drosophila melanogaster*. *FASEB J* 27:288-298.
- 513 Tennessen JM, Bertagnoli NM, Evans J, Sieber MH, Cox J, and Thummel CS. 2014. Coordinated
514 Metabolic Transitions During *Drosophila* Embryogenesis and the Onset of Aerobic
515 Glycolysis. *G3 (Bethesda)*.
- 516 Todorich B, Zhang X, Slagle-Webb B, Seaman WE, and Connor JR. 2008. Tim-2 is the receptor for H-
517 ferritin on oligodendrocytes. *J Neurochem* 107:1495-1505.
- 518 Uhrigshardt H, Rouault TA, and Missirlis F. 2013. Insertion mutants in *Drosophila melanogaster*
519 Hsc20 halt larval growth and lead to reduced iron-sulfur cluster enzyme activities and
520 impaired iron homeostasis. *J Biol Inorg Chem* 18:441-449.
- 521 Wu SC, Liao CW, Pan RL, and Juang JL. 2012a. Infection-induced intestinal oxidative stress triggers
522 organ-to-organ immunological communication in *Drosophila*. *Cell Host Microbe* 11:410-
523 417.
- 524 Wu Z, Du Y, Xue H, Wu Y, and Zhou B. 2012b. Aluminum induces neurodegeneration and its toxicity
525 arises from increased iron accumulation and reactive oxygen species (ROS) production.
526 *Neurobiol Aging* 33:199 e191-112.
- 527 Xu T, and Rubin GM. 1993. Analysis of genetic mosaics in developing and adult *Drosophila* tissues.
528 *Development* 117:1223-1237.
- 529 Zhou G, Kohlhepp P, Geiser D, Frasquillo Mdel C, Vazquez-Moreno L, and Winzerling JJ. 2007. Fate
530 of blood meal iron in mosquitoes. *J Insect Physiol* 53:1169-1178.

cuticle preparation
from ferritin mutants



F

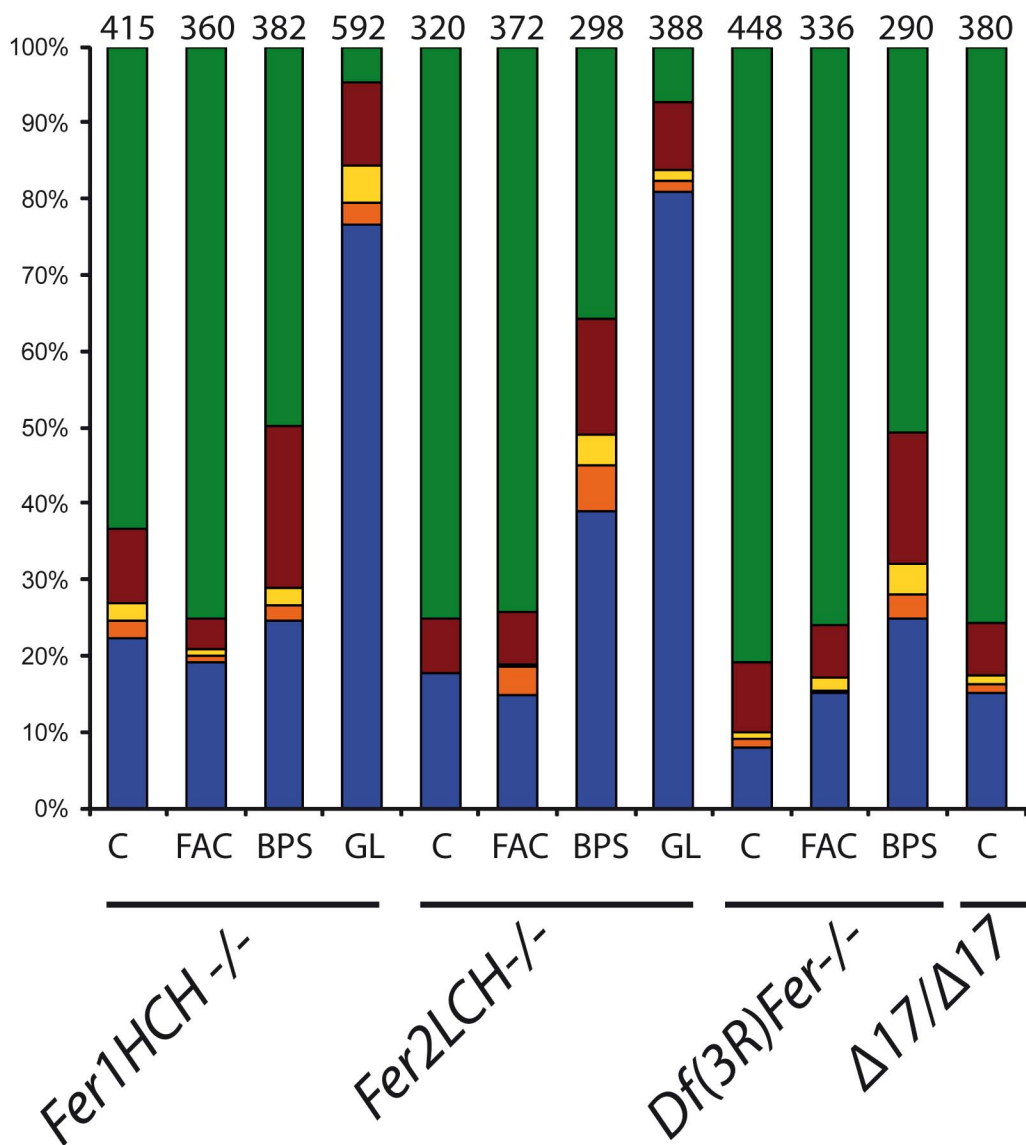


Figure 1

